High Performance Palmprint Identification System Based On Two Dimensional Gabor

I Ketut Gede Darma Putra, Erdiawan
Information Technology, Faculty of Engineering, Udayana University
Bukit Jimbaran, Badung, Bali, Telp. 0361-703315
e-mail : duglaire@yahoo.com

Abstrak

Telapak tangan adalah biometrika yang masih relatif baru. Segmentasi ROI (region of interest) dan ekstraksi fitur telapak tangan merupakan dua isu penting dalam sistem pengenalan telapak tangan. Masalah utama pada sistem pengenalan telapak tangan adalah bagaimana mengekstraksi ROI dan fitur dari telapak tangan. Penelitian ini memperkenalkan metode segmentasi ROI telapak tangan titik pusat moment dua tahap dan kemudian menerapkan metode Gabor dua dimensi (2D) untuk menghasilkan kode telapak tangan (palm code) sebagai fitur telapak tangan. Untuk mengukur tingkat kemiripan dua vektor kode telapak tangan maka digunakan metode jarak Hamming. Pengujian sistem dilakukan dengan menggunakan 1000 sampel telapak tangan milik 200 orang berbeda dengan 3 sampel sebagai sampel acuan dan 2 sampel sebagai sampel uji. Hasil pengujian menunjukkan bahwa sistem mampu menghasilkan unjuk kerja tinggi dengan tingkat keberhasilan mencapai 98.7% (FRR=1.1667%, FAR=0.1111%, T=0.376).

***Kata kunci**: biometrik, jarak hamming, metode Gabor, sistem identifikasi, telapak tangan*

Abstract

The palmprint is a new recognition method in physiological biometrics. In palmprint region of interest (ROI), the segmentation and feature extraction are two important issues. The main problem in palmprint recognition system is how to extract the region of interest (ROI) and the features of palmprint. This paper introduces two steps in center of mass moment and the application of method for ROI segmentation and then to apply the Gabor two dimensional (2D) filters to obtain palm code as palmprint feature vector. Normalized Hamming distance is used to measure the similarity degrees of two feature vectors of palmprint. The system has been tested by using database 1000 palmprint images which was generated from 5 groups of samples from 200 persons selected randomly. Experiment results show that this system can achieve a high performance with success rate about 98.7% (FRR=1.1667%, FAR=0.1111%, T=0.376).

***Keywords**: biometrics, Gabor method, Hamming distance, identification system, palmprint.*

1. Introduction

The personal recognition becomes an important and highly demanded technique for security access systems in this information area, such as: banking, e-commerce, immigration, and court. Palmprint is the relatively new in physiological biometrics.

There are many unique features in a palmprint image that can be used for personal recognition, such as: geometry, principal lines, wrinkles, delta points and minutiae points [1]. A palmprint has several advantages compared to other available features: low-resolution images can be used, low cost capture devices can be used, it is very difficult or impossible to fake palmprint, and their characteristics are stable and unique.

The main problem in palmprint recognition system is how to extract the region of interest (ROI) and the features of palmprint. There were many prior works about palmprint ROI segmentation such as: Li *et al* [2] and Wu *et al* [3] that segmented the palmprint ROI with creating special coordinate axis based on reference points between hand fingers. But creating the special coordinate is relatively difficult. Xiaoxu *at al* develop some key points to generated the ROI [4], Ekinci *et al* [5] repeated the dilation and eriosion morfhology process to extract the

ROI, while Kumar *et al* [6] just repeated erosion process. But repeatedly of morfhology process will increase time complexity of system. This paper proposed new method to extract the ROI of palmprint. This method is called two steps in central moment.

Many researchers were proposed some methods to extract the palmprint features. Zhang *et al* [7], transform the palm lines into set of lines, apply the datum poin characteristics and match the lines by using lines matching technique. Duta *et al* [8] extract set of points along the principals palm lines and compute the score between two relates features (points) of palmprint. Li *et al* apply Fourier transform on palmprint and used *ring energy and sector energy* to form the palmprint features. Wu *et al* [9] used *directional element feature* (DEF) fo determine *fuzzy directional element energy feature* (FDEEF). Two types of low dimension feature can be derived from FDEEF, namely: global *fuzzy directional element energy feature* (GFDEEF) and *block edge energy feature* (BEEF), and than Euclidean distance is used to match two palmprint features. Ekinci *et al* form *elational graph* from palm lines and based on the graph is created *adjacent unit matrix* for classification process. Xiaoxu *at al* extracted the the texture feature of palmprint based on kernel principal component analysis (K-PCA). Wu *et al* extract *line vector features* (LVF) based on gradien magnitudo and orientation points on the palm lines. Kumar *et al* detect the palm lines in special direction and the feature are devided into sub blocks and the feature is obtained by computing the standard deviation of each block. We also tried some methods to extract the palmprint features, such as: wavelet [10], fractal dimension and fractal code [11], [12]. This paper apply Gabor 2D filter to obtain the palmprint features or palmcode

2. Research Method

2.1 Hand image Acquisition

All of palm images are captured using Sony DSC P72 digital camera with resolution of 640x480 pixels. Each person was requested to put his/her left hand palm down on with a black background (five samples for each person). There are some pegs on the board to control the hand oriented, translation, and stretching as shown in Figure 1.

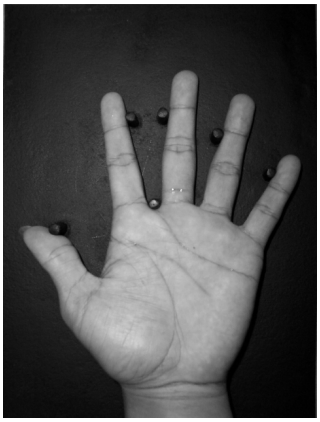

Figure 1. Hand image acquisition

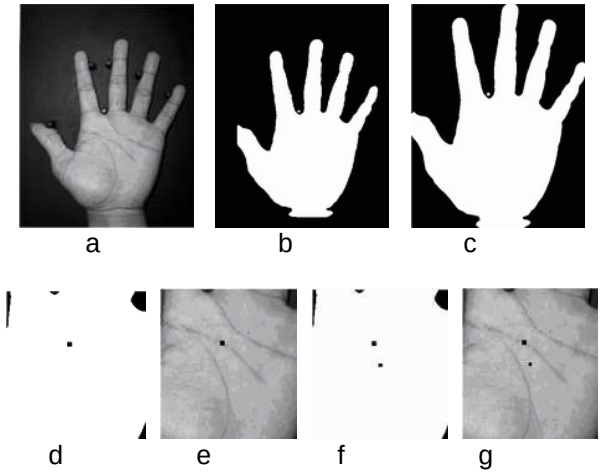

Figure 2. Extraction of palmprint, (a) original image, (b) binary image of (a), (c) object bounded, (d) and (e) position of the first centroid mass in segmented binary and gray level image, respectively, (f) and (g) position of the second centroid mass in segmented binary and gray level image, respectively.

2.2 Segmentation of Palmprint ROI

Segmentation of palmprint ROI is one of important factor for recognition performance. This paper proposed new technique to extract the ROI is called two steps in moment central method. The steps of the method can be explained as follow:

a. The gray level hand image is threshold to obtain the binary hand image. The threshold value is computed automatically using the Otsu method. To avoid the white pixels (not pixel object) outside of the hand object is used median filter.
b. Each of the acquired hand images needs to be aligned in a preferred direction so as to capture the same features for matching. The moment orientation method is applied to the binary image to estimate the orientation of the hand. In the method, the angle of rotation (θ) is the difference between normal axis and major axis of ellipse that can be computed as follows.

$$\theta = \frac{1}{2}\tan^{-1}\left[\frac{2\mu_{1,1}}{\mu_{2,0}-\mu_{0,2}}\right] \quad (1)$$

$$\mu_{p,q} = \sum_m \sum_n (m-\overline{m})^p (n-\overline{n})^q \quad (2)$$

Where $\mu_{p,q}$ represent the (p,q)th moment central, and ($\overline{m},\overline{n}$) represents center of area is defined as

$$\overline{m} = \frac{1}{N}\sum_m \sum_n m\,,\ \overline{n} = \frac{1}{N}\sum_m \sum_n n\,, \quad (3)$$

Where *N* represent number of pixel object. Furthermore, the grayscale and the binary image are rotated about (θ) degree.
c. Bounding box operation is applied to the rotated binary image to get the smallest rectangle which contains the binary hand image. The original hand image, binarized image, and the bounded image shown in Figure 2 (a), (b), and (c), respectively.
d. The centroid of bounded image is computed using equation (3) and based on this centroid, the bounded binary and original images are segmented with 200x200 pixels. The segmented image and its centroid position are shown in Figure 2 (d) and (e).
e. The centroid of the segmented binary image is computed and based on this centroid the ROI of grayscale palmprint image can be cropped with size 128x128 pixels. The first and the second positions of centroid in binary and gray level image are shown in Figure 1 (f) and (g).

This method is simple. This method has been tested for 1000 palmprint images acquired from 200 persons, and the results show this method is reliable.

2.3 Palmprint Normalization

The normalization process is needed to reduce the possible imperfections in the palmprint image due to non-uniform illumination. The normalization method employed in this research as follow:

$$I'(x,y) = \begin{cases} \phi_d + \lambda & if\ I(x,y) > \phi \\ \phi_d - \lambda & otherwise \end{cases} \quad (4)$$

$$\lambda = \sqrt{\frac{\rho_d \{I(x,y)-\phi\}^2}{\rho}} \quad (5)$$

where *I* and *I'* represents original grayscale palmprint image and the normalized image respectively, ϕ and ρ represents mean and variance of the original image respectively, while ϕ_d and ρ_d are the desired values for mean and variance respectively. This research use ϕ_d = 180 and ρ_d = 180 for all experiments, and the results are shown in Figure 3.

2.4 Palmprint Feature Extraction

Palmprint features are obtained by using 2D Gabor filter. The filters can be produced using the equation below:

$$G(x,y,\theta,u.\sigma)=\frac{1}{2.\pi.\sigma^2}\exp\left\{-\frac{x^2+y^2}{2.\sigma^2}\right\}\exp\{2.\pi.i(u.x.\cos\theta+u.y.\sin\theta)\} \quad (6)$$

where, $i=\sqrt{-1}$, u is frequency of the sinusoidal wave. θ is control of the orientation of Gabor function. σ is standard deviation of the envelope Gaussian. x, y is coordinates of Gabor filters.

The normalized Gabor filters can be obtained by using the following equation.

$$\tilde{G}[x,y,\theta,u,\sigma]=G[x,y,\theta,u,\sigma]-\frac{\sum_{i=-n}^{n}\sum_{j=-n}^{n}G[i,j,\theta,u,\sigma]}{(2n+1)^2} \quad (7)$$

With $(2n+1)^2$ is the size of the Gabor filter. In fact, the imaginary part of Gabor filter automatically has zero DC because of odd size filters. It should be noted that the success of Gabor filter depend on parameters θ, σ, u selection for these filters.

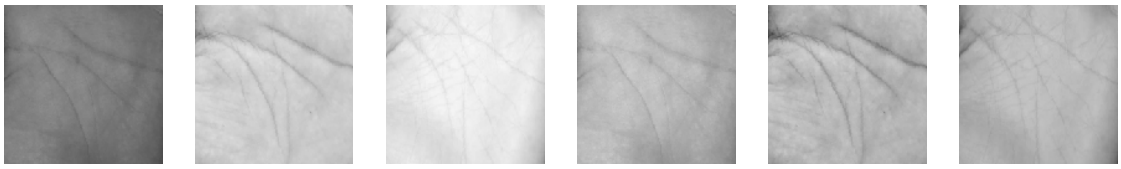

a b c d e F

Figure 3. Intensity normalization results, (a, b, c) the original images with different lighting, (d, e, f) normalization results with ϕ_d=180 and ρ_d=180

The equation (6) and (7) will produce variously of Gabor filter that consist of real and imaginary parts. The parameters value of θ,σ,u and filter size will impact of performance of Gabor filter. This research used the Gabor filter size: 9x9, 17x17 and 35x35, with value of θ are -45°, 0°, 45° and 90°, while value of u and σ were appropriated with filter size.

Real and imaginary part of normalized Gabor filters are convoluted to the normalized palmprint images and produces real and imaginary characteristic features with equal size to the original palmprint size.

2.5 Generating Palmcode

Palmcode is binary and unique codes that obtained from real and imaginary features of palmprint. Palmcode can be generated by using the rules below:

$$\begin{aligned} br&=1 \text{ if } \mathrm{Re}[\tilde{G}[x,y,\theta,\sigma]*I]\geq 0 \\ br&=0 \text{ if } \mathrm{Re}[\tilde{G}[x,y,\theta,\sigma]*I]<0 \\ bi&=1 \text{ if } \mathrm{Im}[\tilde{G}[x,y,\theta,\sigma]*I]\geq 0 \\ bi&=0 \text{ if } \mathrm{Im}[\tilde{G}[x,y,\theta,\sigma]*I]<0 \end{aligned} \quad (8)$$

Where, *I* represent normalized palmprint image and * is convolution operator.

a b c d e f

Figure 4. Palmcodes with various filter size real and imaginary codes respectively with, (a)-(b) 9x9 filter size, (c)-(d) 17x17 filter size, (e)-(f) 35x35 filter size.

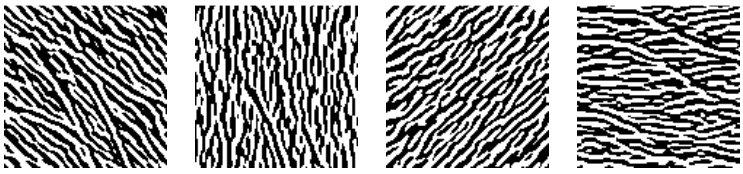

a b c d

Figure 5. The real part of palmcode with 17x17 filter size by using: (a) -45°, (b) 0°, (c) 45°, and (d) 90°.

Palmcode examples with orientation 45^o and different in filter size, such as 9x9, 17x17 and 35x35 is shown in Figure 4, while Figure 5 show the palmcodes with filter size 17x17 and different in orientation angle, such as -45^o, 0^o, 45^o and 90^o.

2.6 Palmcode Matching

Palmcode matching aimed to obtain similarity degree between two palmcode. The similarity degree is noted as score. This paper used normalized Hamming distance. The distance of two palmcode P and Q can be computed as follows:

$$D_O = \frac{\sum_{i=1}^{N}\sum_{j=1}^{N}\left(P_R(i,j) \otimes Q_R(i,j)\right) + \left(P_I(i,j) \otimes Q_I(i,j)\right)}{2N^2} \quad (9)$$

Where $P_R(Q_R)$ and $P_I(Q_I)$ represents real and imaginary parts of palmcode $P(Q)$. Operator *Boolean* $(\otimes)$ produces zero value if and only if bit of $P_{R(I)}(i,j)$ and $Q_{R(I)}(i,j)$ is equal. Matrix size is noted by NxN. The range of score D_0 is between 0 and 1. The score will be closed to 0 if two palmcodes come from the similar palmprint, otherwise, the score will be far from 0. One of palmcode can be translated in both vertical and horizontal direction with one or more pixels to minimize the impact of imperfectness at image preprocessing or acquisition phase. The minimum score from the translated palmcode matching process is selected as score of matching. Threshold value (T) is used to decide the tested palmcode is genuine or impostor. If the score less than or equal with T then the tested palmcode is noted as authorized, otherwise the palmcode is noted as not authorized.

3. Results and Analysis

Those methods have been applied for palmprint identification system. The system is tested using database of 1000 palmprint images, are generated from 5 samples from each of the 200 persons randomly selected. The first three images from each user were used for training and the rest were used for testing, so the total number of testing and training image are 400 and 600 respectively. The performance of the identification system is obtained by matching each of testing palmprint images with all of the training palmprint images in the database. A matching is noted as a correct matching if the two palmprint images are from the same palm and as incorrect if otherwise. This paper used FAR (false acceptance rate), FRR (false rejection

rate), system accuracy, genuine and imposter score distribution graphics, and *receiver operation curve* (ROC) as indicators of the performance system.

The genuine and imposter scores are obtained from the matching scores of same person and different person respectively. There were not zero scores that produced from the matching process that means all palmprint samples that are used in this experiment are different.

This paper used parameter values below to test the system:

ROI size = 64x64 and 128x128 *pixels*
Filter size = 9x9, 17x17, and 35x35
θ = -45°, 0°, 45° and 90°.
u , σ = 0.3666, 1.4045 for 9x9 filter
0.1833, 2.8090 for 17x17 filter
0.0916, 5.619 for 35x35 filter

and the translation factors are without translation and 1 pixel translation.

Table 1. The best accuracy rate (in %) of ROI 64x64 *pixel*, N=100

θ	filter 9x9		filter 17x17		filter 35x35	
	A	B	A	B	A	B
-45°	70.03	96.95	88.22	97.64	90.65	95.67
0°	82.25	96.19	94.59	98.45	94.91	97.18
45°	80.08	92.99	96.44	**98.72**	96.82	97.29
90°	67.23	93.69	87.14	97.69	92.75	96.82

Table 2. The best accuracy rate (in %) of ROI 128x128 *pixel*, N=100

θ	filter 9x9		filter 17x17		filter 35x35	
	A	B	A	B	A	B
-45°	51.44	89.05	71.29	93.62	88.47	95.79
0°	61.26	87.25	85.61	95.30	94.80	97.51
45°	62.26	85.74	84.76	94.61	96.19	**98.46**
90°	56.77	73.14	71.09	88.33	87.11	95.05

The column A and B represent system accuracy rate (in %) without or with 1 pixel translation. Table 1 and Table 2 show that the filter size 9x9 produced the lowest accuracy rate than 17x17 and 35x35 and translation factor 1 pixel produced better accuracy rate than without translation factor. The 1 pixel translation factor can minimized the impact of imperfectness in ROI segmentation.

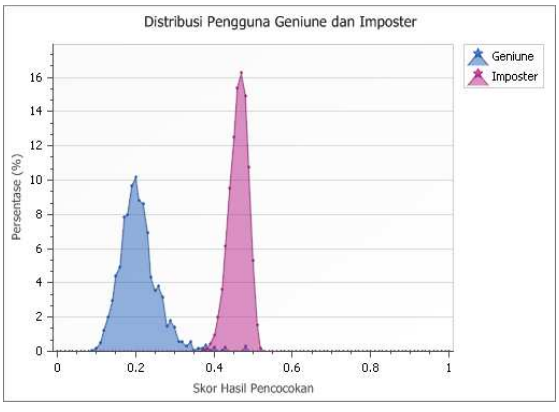

Figure 6. Genuine and imposter score distribution with filter 17x17, orientation 45°, ROI 64x64 *Pixel*, 1 *Pixel* translation, and N=200

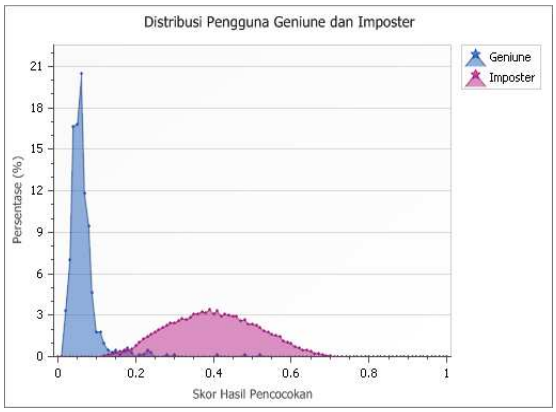

Figure 7. Genuine and imposter score distribution with filter 35x35, orientation 45°, ROI 64x64 *Pixel*, 1 *Pixel* translation, and N=200

Figure 6 and Figure 7 show distribution scores of genuine and impostor at database with size N=200 for ROI 64x64, by using filter size 17x17 and 35x35, orientation -45^{o} and translation factor 1 *pixel*. The axis in those figures represents scores value and y axis represent percentages of appropriate score appear. If overlapping part of both graphics increase then performance of the system will be decrease, and vice versa.

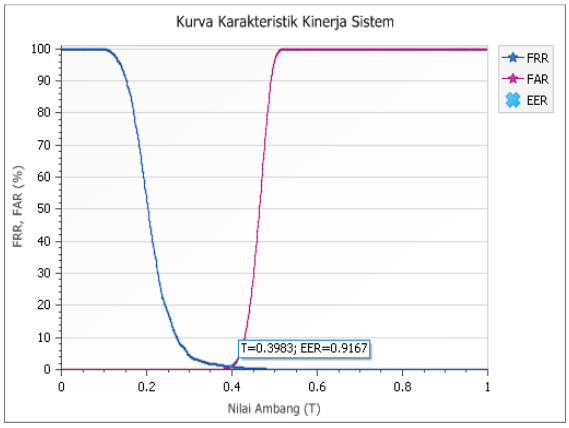

Figure 8. ROC system with filter 17x17, orientation 45°, ROI 64x64 *pixel*, 1 *pixel* translation, and N=200

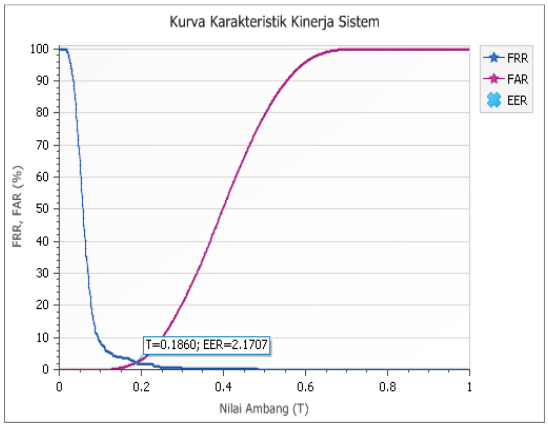

Figure 9. ROC system with filter 35x35, orientation -45°, ROI 64x64 *pixel*, 1 *pixel* translation, and N=200

The *receiver operation curve* (ROC) of Figure 6 and 7 are shown in Figure 8 and 9 respectively. The axis of ROC represents *threshold value* (T), while y axis represents percentages of FRR and FAR. Cross point of FAR and FRR curves produce EER (*equal error rate*) value. The system produced FAR=FRR=EER=0.9167 with appropriate T=0.3983 (as shown in Figure 8), and produced FAR=FRR=EER=2.1707 with appropriate T=0.1860 (as shown in Figure 9). FAR and FRR system depend on selecting of threshold value. Increasing FAR and FRR system will decrease performance of system, and vice versa. FAR and FRR will be increase If overlapping part of genuine and imposter scores distribution increases.

Distribution scores and ROC graphics of filter size 9x9 are not shown in this paper is based on consideration its performances is lower than others filter size, and also distribution scores and ROC of the system without translation factor is lower than with 1 pixel translation factor so their graphics is hidden.

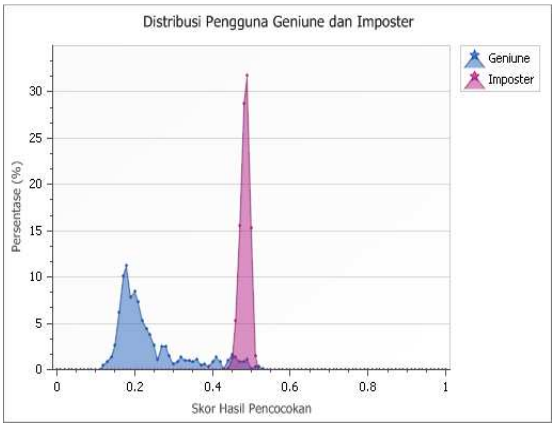

Figure 10. Genuine and imposter score distribution with filter 17x17, orientation -45°, ROI 128x128 *Pixel*, 1 *Pixel* translation, and N=200

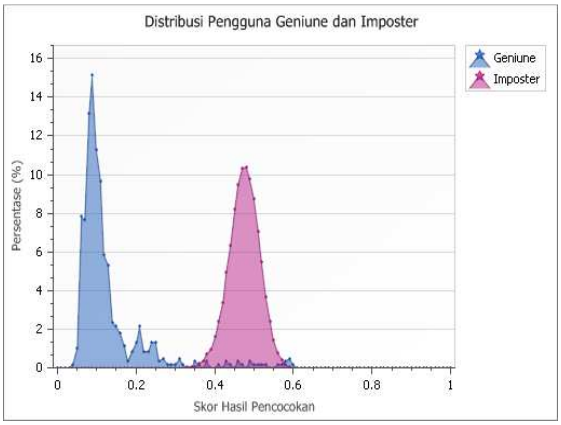

Figure 11. Genuine and imposter score distribution with filter 35x35, orientation -45°, ROI 128x128 *Pixel*, 1 *Pixel* translation, and N=200

Figure 10 and 11 show distribution scores of genuine and impostor on database size N=200 for ROI 128x128, by using filter size 17x17 and 35x35, orientation -45^{o} and translation factor 1 *pixel*, while its ROC curves are shown in Figure 12 and 13 respectively. Increasing the overlapping part of score distribution (as shown in Figure 10 and 11) will increase the FAR, FRR and EER value (as shown in Figure 12 and 13).

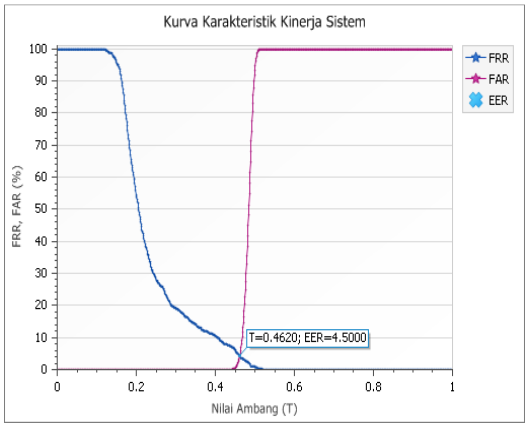

Figure 12. ROC system with filter 17x17, orientation -45°, ROI 128x128 pixel, 1 pixel translation, and N=200

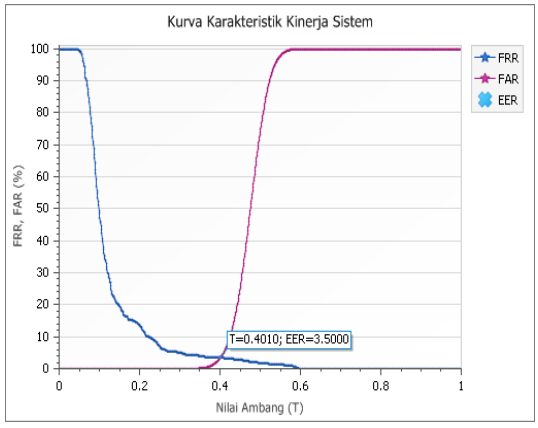

Figure 13. ROC system with filter 35x35, orientation -45°, ROI 128x128 pixel, 1 pixel translation, and N=200

System testing using various database sizes is shown in Table 3 and 4, while its graphics are shown in Figure 14.

Table 3. System performance with ROI 64x64 *pixel* on various database sizes

Database size (in user)	filter 17x17		filter 35x35	
	A	B	A	B
25	99.5278	100	98.6667	98.1111
50	96.0272	99.1973	96.4286	97.0544
75	96.2913	98.5916	96.4354	97.1321
100	96.4444	98.7222	96.8215	97.2997
125	95.8495	98.3871	96.5914	97.4710
150	95.5272	98.6033	96.4937	97.2834
175	95.8714	98.6398	96.7499	97.2830
200	96.0105	**98.7877**	96.8848	97.2839

Table 4. System performance with ROI 128x128 *pixel* on various database sizes

Database size (in user)	filter 17x17		filter 35x35	
	A	B	A	B
25	94.1944	100	100	100
50	86.1633	94.6803	95.7415	98.5850
75	84.4535	93.8649	96.1471	98.1862
100	84.7559	94.6094	96.1936	98.4596
125	83.3516	93.6591	96.3290	98.4645
150	82.4787	94.2081	95.8098	98.7040
175	83.5063	94.6086	96.1166	98.6897
200	84.4389	94.8978	96.2630	**98.7910**

Table 3 show that by using ROI 64x64, performance of the system that obtained by using filter size 17x17 is better than filter size 35x35 relatively, while in table 4 show vice versa, by using ROI 128x128, filter size 35x35 is better than filter size 17x17 relatively. The best performance of both ROI *achieve* 98.7% by using filter size 17x17 on ROI 64x64, and filter size 35x35 on ROI 128x128, and both of them used 1 pixel translation factor.

Figure 14 is made based on data in Tables 3 and 4. The Figure show, both ROI 64x64 and 128x128, the performance (accuracy) of the system is relatively stable although size of database increased. This is a good information to apply the palmcode on large scale database.

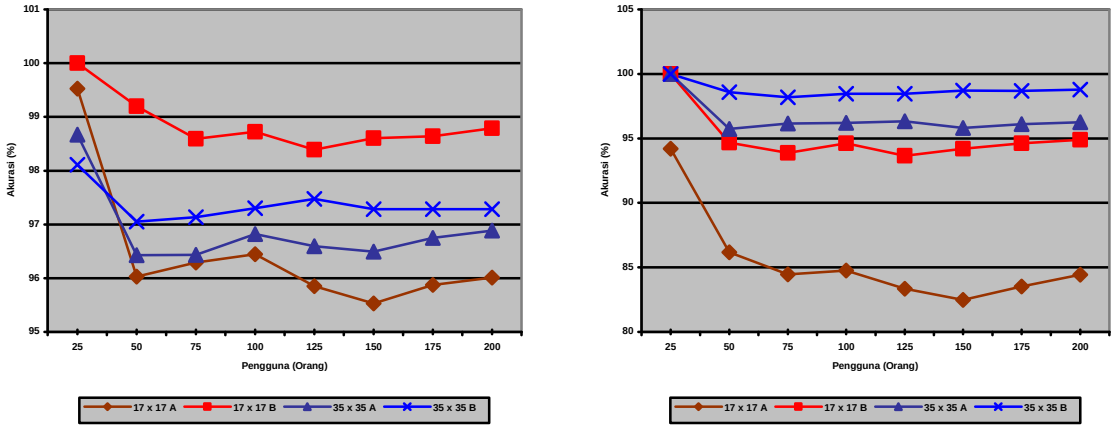

(a) (b)

Figure 14. Impact of increasing of database size to the accuracy system (a) ROI 64x64 *pixels*, (b) ROI 128x128 *pixels*

Table 1. Time complexity using N=200

Operation	Time (seconds) filter 17x17 ROI 64x64	filter 35x35 ROI 128x128	Ratio
Preprocessing	0.81	0.81	1 : 1
Feature Extraction	0.1602	2.7039	1 : 17
Palmcode Matching (translation 1 *pixel*)	6.6596	24.1347	1 : 4

Time complexity on Table 5 is obtain by using Pentium III Intel 733 MHz, 512 MB RAM.

4. Conclusion

The proposed two steps in central moments method for ROI of palmprint extraction and the applied of Gabor filter for palmcode generation produced high performance for palmprint identification system with accuracy rate reached 98.7% or FAR=0.111% and FRR=1.167%. The appropriate parameters value to obtain the above performance are: 17x17 in filter size on ROI size 64x64 pixel, and 35x35 in filter size on ROI 128x128, and both of them used θ=45° and 1 pixel translation factor. The experiment result also show that the performance of this system relatively stable although the database size increased.

This research just developed offline recognition system. The online palmprint recognition system from hardware device to software recognition system and apply the system in to a public application, such as smartcard and ID card are interesting research for future.

References

[1] Shu W., Zhang D., Automated personal identification by palmprint, *Optical Engineering, 1998;* 37(8): 2359-2363.
[2] LI Wen-xin, David Z,, Shuo-qun XU., Palmprint Recognition Based on Fourier Transform, *Journal of Software, 2002; 13(5): 879-886*
[3] WU Xiang-Quan, Kuan-Quan Wang, David Zhang, An Approach to Line Feature Representation and Matching for Palmprint Recognition, *Journal of Software,* 2004; 15(6): 869-880

[4] Xiaoxu Cheng, Shuhua Wang, *A New Palmprint Identification Technique Based On a Two-stage Neural Network Classifier*, International Conference on Computer Science and Software Engineering, Hubei, China, 2008: 957-960
[5] Ekinci M., Vasif V., Nabiyev, Yusuf Ozturk, A Biometric Personal Verification Using Palmprint Structural Features and Classifications, *IJCI Proceedings of Intl XII, Turki, 2002; 1(1)*
[6] Kumar A., David C.M.Wong, Helen C.Shen, Anil K.Jain, *Personal Verification using Palmprint and Hand Geometry Biometric*, 4th International Conference on Audio-and Video-Based Biometric Person Authentication, Guildform, UK 2003
[7] Zhang D., and W.Shu, 1999, "Two novel characteritics in palmprint verification: datum point invariance and line feature matching", *Pattern Recognition*, 1998; *32: 691-702*
[8] Duta N., Jain A.K., Mardia K.V., Matching of Palmprints, *Pattern Recognition Letters,* 2002; 23: *477-485*
[9] Wu, X., K.Wand, D.Zhang, Fuzzy directional element energy feature (FDEEF) based palmprint identification, proceedings 16th International Conferences on pattern recognition*, Quebec, 2002; 1: 95-98*
[10] Darma Putra, IKG. Metode Fraktal untuk Sistem Pengenalan Biometrika Telapak Tangan. Disertasi. Yogyakarta: Pascasarjana UGM; 2007.
[11] Darma Putra, Adhi Susanto, Agus Harjoko, Thomas Sri Widodo, Identifikasi Telapak Tangan dengan Memanfaatkan Alihragam Gelombang Singkat, *Jurnal Terakreditasi PAKAR,* 2004; *5(3) :161-172*
[12] Darma Putra, IKG., Adhi Susanto, A. Harjoko & TS. Widodo, Palmprint Verification based on fractal Codes and Fractal Dimensions, *Proceedings of the Eighth IEASTED International Conference Signal and Image Processing,* Honolulu, Hawai, 2006; 323–328.